

5

SEMI-ANNUAL TECHNICAL REPORT NO. 2

1 December 1983 - 31 May 1984

"Influence of Scattering on Q in the Lithosphere"

By

Anton M. Dainty

School of Geophysical Sciences  
Georgia Institute of Technology  
Atlanta, Georgia 30332

Principal Investigator: Anton M. Dainty (404) 894-2860

Contract Amount: \$85,000

Contract Termination Date: 14 November 1984

Program Manager: William J. Best (202) 767-4908

Sponsored by

Advanced Research Projects Agency (DOD)

ARPA Order No. 4397, Am No. 3

Monitored by NP Under Grant No. AFOSR-83-0037

Program Code: 3D60

Approved for public release;  
distribution unlimited.

DTIC  
ELECTE

JAN 2 1985

A

The views and conclusions contained in this document are those of the author and should not be interpreted as necessarily representing the official policies, either expressed or implied, of the Defense Advanced Research Projects Agency or the U.S. Government.

AD-A149 318

DTIC FILE COPY

UNCLASSIFIED

SECURITY CLASSIFICATION OF THIS PAGE

## REPORT DOCUMENTATION PAGE

1a. REPORT SECURITY CLASSIFICATION <b>UNCLASSIFIED</b>			1b. RESTRICTIVE MARKINGS														
2a. SECURITY CLASSIFICATION AUTHORITY			3. DISTRIBUTION/AVAILABILITY OF REPORT														
2b. DECLASSIFICATION/DOWNGRADING SCHEDULE			Approved for public release; distribution unlimited.														
4. PERFORMING ORGANIZATION REPORT NUMBER(S)			5. MONITORING ORGANIZATION REPORT NUMBER(S) <b>AFOSR-TR- 84-1157</b>														
6a. NAME OF PERFORMING ORGANIZATION Georgia Tech Research Institute		6b. OFFICE SYMBOL (If applicable)	7a. NAME OF MONITORING ORGANIZATION Air Force Office of Scientific Research														
6c. ADDRESS (City, State and ZIP Code) Atlanta, GA 30332			7b. ADDRESS (City, State and ZIP Code) Bolling Air Force Base Washington, DC 20332														
8a. NAME OF FUNDING/SPONSORING ORGANIZATION Defense Advanced Research Projects Agency		8b. OFFICE SYMBOL (If applicable)	9. PROCUREMENT INSTRUMENT IDENTIFICATION NUMBER AFOSR-83-0037														
8c. ADDRESS (City, State and ZIP Code) 1400 Wilson Boulevard Arlington, VA 27709			10. SOURCE OF FUNDING NOS.														
			<table border="1"><tr><td>PROGRAM ELEMENT NO. <b>41101E</b></td><td>PROJECT NO. <b>A0</b></td><td>TASK NO. <b>08</b></td><td>WORK UNIT NO.</td></tr></table>			PROGRAM ELEMENT NO. <b>41101E</b>	PROJECT NO. <b>A0</b>	TASK NO. <b>08</b>	WORK UNIT NO.								
PROGRAM ELEMENT NO. <b>41101E</b>	PROJECT NO. <b>A0</b>	TASK NO. <b>08</b>	WORK UNIT NO.														
11. TITLE (Include Security Classification) Investigation of Scattering and Q in the Lithosphere (UNCLASSIFIED)																	
12. PERSONAL AUTHOR(S) Anton M. Dainty																	
13a. TYPE OF REPORT Semi-Annual Technical		13b. TIME COVERED FROM 83/12/01 TO 84/05/31		14. DATE OF REPORT (Yr., Mo., Day)													
15. PAGE COUNT																	
16. SUPPLEMENTARY NOTATION																	
17. COSATI CODES																	
<table border="1"><tr><td>FIELD</td><td>GROUP</td><td>SUB. GR.</td></tr><tr><td></td><td></td><td></td></tr><tr><td></td><td></td><td></td></tr><tr><td></td><td></td><td></td></tr></table>						FIELD	GROUP	SUB. GR.									
FIELD	GROUP	SUB. GR.															
18. SUBJECT TERMS (Continue on reverse if necessary and identify by block number)																	
19. ABSTRACT (Continue on reverse if necessary and identify by block number)  Codas of local earthquakes from Monticello Reservoir, South Carolina, and Mammoth Lakes, California, have been examined to determine scattering parameters and attenuation for the crust in these areas. The backscattering turbidity (or backscattering cross-section per unit volume) and the total coda Q have been determined. In both areas, strong scattering is observed in the near surface crust (upper 10 km), sufficiently strong that multiple scattering is occurring. Because multiple scattering is occurring, coda Q at short times will underestimate Q experienced by a short pulse. At long times, the coda at Monticello indicates the presence of a low-scattering crustal channel within which energy probably spreads horizontally; this channel is either absent or (Continued)																	
20. DISTRIBUTION/AVAILABILITY OF ABSTRACT UNCLASSIFIED/UNLIMITED <input checked="" type="checkbox"/> SAME AS RPT. <input type="checkbox"/> DTIC USERS <input type="checkbox"/>			21. ABSTRACT SECURITY CLASSIFICATION UNCLASSIFIED														
22a. NAME OF RESPONSIBLE INDIVIDUAL		22b. TELEPHONE NUMBER (Include Area Code)		22c. OFFICE SYMBOL													

more strongly scattering at Mammoth Lakes. Results at both sites indicate that both in the near surface region and in the aforementioned crustal channel, scattering is probably an important contributor to Q (at least half of the attenuation). The scatterers are probably predominantly forward scattering (such as velocity fluctuations), and in the near surface there are many scatterers of size 50 m and greater.

Accession For	
NTIS GRA&I	<input checked="checked" type="checkbox"/>
DTIC TAB	<input type="checkbox"/>
Unannounced	<input type="checkbox"/>
Justification	
By	
Distribution/	
Availability Codes	
Dist	Avail and/or Special
A-1	

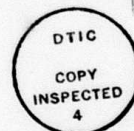




## TABLE OF CONTENTS

	<u>Page</u>
1. Technical Report Summary . . . . .	1
2. Long and Short Codas in California and South Carolina. . . . .	2

AIR FORCE OFFICE OF SCIENTIFIC RESEARCH (AFSC)  
NOTICE OF TRANSMITTAL TO DTIC  
This technical report has been reviewed and is  
approved for public release JAN APR 190-12.  
Distribution is unlimited.  
MATTHEW J. KEEPER  
Chief, Technical Information Division

TABLE OF CONTENTS

	<u>Page</u>
1. Technical Report Summary . . . . .	1
2. Long and Short Cotas in California and South Carolina. . . . .	2

AIR FORCE OFFICE OF SCIENTIFIC RESEARCH (AFSC)  
NOTICE OF 1941  
This technical report is  
approved for release to the public  
Distribution is unlimited  
MATTHEW J. [illegible]  
Chief, Technical Information Division

## TECHNICAL REPORT SUMMARY

Codas of local earthquakes from Monticello Reservoir, South Carolina, and Mammoth Lakes, California, have been examined to determine scattering parameters and attenuation for the crust in these areas. The backscattering turbidity (or backscattering cross-section per unit volume) and the total coda  $Q$  have been determined. In both areas, strong scattering is observed in the near surface crust (upper 10 km), sufficiently strong that multiple scattering is occurring. Because multiple scattering is occurring, coda  $Q$  at short times will underestimate  $Q$  experienced by a short pulse. At long times, the coda at Monticello indicates the presence of a low-scattering crustal channel within which energy probably spreads horizontally; this channel is either absent or more strongly scattering at Mammoth Lakes. Results at both sites indicate that both in the near surface region and in the aforementioned crustal channel, scattering is probably an important contributor to  $Q$  (at least half of the attenuation). The scatterers are probably predominantly forward scattering (such as velocity fluctuations), and in the near surface there are many scatterers of size 50 m and greater.

## LONG AND SHORT CODAS IN CALIFORNIA AND SOUTH CAROLINA

### Introduction

This report is a follow-up report to an earlier study (Dainty and Tie, 1984) in which the local coda of some aftershocks of the May 25 and 27, 1980, earthquake near Mammoth Lakes, California, were analyzed. This analysis indicated that for coda lengths of 10 seconds or less, the scattering implied by the decay of the coda was not consistent with the scattering implied by the amplitude of the coda relative to the amplitude of the direct S wave. Briefly, the scattering implied by the coda amplitude should lead to more rapid decay of the coda than is observed at frequencies around 3 Hz, if the single scattering theory used to analyze the data is correct.

I have examined other local earthquake records to see if the results presented above are correct for these codas. Besides records of length 10 seconds or less, I have analyzed records of substantially longer length to see if the effects are seen at longer times. Different records from Mammoth Lakes (Archuleta et al., 1982), analyzed by a different investigator, and records from Monticello Reservoir, South Carolina (Fletcher, 1982), will be used. These are the records analyzed by Duckworth (1983) and Dainty and Duckworth (1983).

### Theoretical Summary: Single Scattering and Multiple Scattering

The standard theory used to analyze codas is the single scattering theory due to Aki, summarized in Aki and Chouet (1975). This theory has been used in earlier reports. The theory assumes a whole space in which

scatterers are distributed randomly. These scatterers may be approximated by some body of specified geometrical shape or may be defined by their autocorrelation functions. Since an elastic medium has (at least) three independent relevant material constants, two elastic constants and density, the three quantities must be specified, although we expect some correlation between the three quantities. Generally, it has been assumed that only S to S scattering is important, but recent results by Wu and Aki (1984) suggest that S to P scattering could also be important. P to P and P to S scattering would be less important because earthquakes do not generate as much P as S.

Briefly, the theory alluded to implies that at long times the coda power spectrum shall decay with time  $t$  after origin as

$$P_c(\omega, t) = A_b(\omega) t^{-2} \exp(-\omega t/Q) \quad (1)$$

$$A_b(\omega) = P_s(\omega) \cdot \exp(\omega t_s/Q) \cdot 8\pi V \cdot g(\pi, \omega) \cdot t_s^2 \quad (2)$$

$$1/Q = 1/Q_i + 1/Q_s \quad (3)$$

$$1/Q_s = G(\omega) V/\omega \quad (4)$$

$P_s(\omega)$  is the square of the S wave spectrum,  $V$  is the seismic velocity (assumed to be 3.2 km/sec, typical of S waves in the crust, in this study),  $t_s$  is the S travel time,  $Q_i$  is the  $Q$  due to anelasticity, and  $Q_s$  is the  $Q$  due to scattering. The scattering is described by two parameters. The backscattering turbidity  $g(\pi, \omega)$  or backscattering cross section per unit volume describes the strength of backscattering and controls the amplitude of the coda relative to the amplitude of the S wave, as seen in (2). The total turbidity  $G(\omega)$ , or total cross-section



per unit volume, describes the strength of total scattering in all directions and controls the  $Q$  due to scattering through (4). Another parameter that I have calculated is the apparent total turbidity

$$G_a(\omega) = \frac{\omega}{QV} \quad (5)$$

If the intrinsic attenuation can be neglected, the apparent total turbidity is the same as the total turbidity. Generally, in single scattering,

$$G_a(\omega) \geq G(\omega) \geq g(\pi, \omega) \quad (6)$$

So far, the theoretical discussion has assumed that the coda consists of scattered body waves of one type in a whole space. In view of the results to be presented casting doubt on this, some other possibilities must be discussed. The simplest is the case of singly scattered surface waves, rather than body waves, from a near surface source: Equation (1) becomes

$$P_c(\omega, t) = A_s(\omega) t^{-1} \exp(-\omega t/Q) \quad (7)$$

$$A_s(\omega) = P'_s(\omega) \cdot \exp(\omega t'_s/Q) \cdot 2\pi V' \cdot g'(\pi, \omega) \cdot t'_s \quad (8)$$

$$1/Q = 1/Q'_i + G'(\omega)V'/\omega \quad (9)$$

The primed quantities in (8) and (9) indicate that these variables have the same definitions as before, but for surface waves rather than S waves. Another possibility is of two or more singly scattered "channels" for the transmission of energy that appears in the coda--for

example, one channel could be body wave scattering and the other surface wave scattering. Then the coda power spectrum would become

$$P_c(\omega, t) = P_1(\omega, t) + P_2(\omega, t) \quad (10)$$

where  $P_1$  and  $P_2$  are the contributions from each channel.

Another important issue is that of multiple scattering as opposed to single scattering. Dainty and Toksöz (1977) demonstrated that in the limit of extreme multiple scattering, seismic energy diffuses. The coda power spectrum for a point, impulsive source in a whole space then becomes (Dainty and Toksöz, 1981):

$$P_c(\omega, t) = E_b(\omega) t^{-3/2} \exp[-3R^2 G(\omega)/(4Vt)] \exp[-\omega t/Q_i] \quad (11)$$

$$\rightarrow E_b(\omega) t^{-3/2} e[-\omega t/Q_i], \quad R \rightarrow 0 \quad (12)$$

$$E_b(\omega) = P_s(\omega) \cdot \sqrt{27G^3(\omega)} / (8\sqrt{\pi^3 V^3}) \quad (13)$$

Here  $R$  is the source-receiver distance, taken to be small in (12). Note that (12) is rather similar to (1) or (7) in that it indicates that at a fixed frequency, for short source-receiver distance (the usual experimental situation), the coda power spectrum should decay with time as the product of an inverse power law intermediate between (1) and (7) and an exponential. Thus if an attempt was made to fit equation (1) or (7) to a situation in fact described by equation (12), an apparently good fit would be obtained. However, the interpretation of the parameters would change. In (12), the exponential decay gives the value of  $Q_i$ , the intrinsic attenuation, and not  $Q$  as defined by (3) or (9). In fact,

$$Q_i \geq Q \quad (14)$$

I will assume that the general effect of multiple scattering is to increase the value of  $Q$  measured as compared to that implied by (3) or (9). This will decrease  $G_a(\omega)$  calculated from (5).

In this paper  $g(\pi, \omega)$  has been calculated from (2) or (8), i.e., under the assumption of single scattering. Essentially, this means that  $g(\pi, \omega)$  has been calculated from the ratio of the coda power to the  $S$  wave power, with a (variable) factor. From (13), this ratio should be large for the case of multiple ("strong") scattering, since  $G(\omega)$  will be large; thus large values of  $g(\pi, \omega)$  should be found. Combined with this result with the result for  $G_a(\omega)$  just discussed, increasing  $g(\pi, \omega)$  and simultaneously decreasing  $G_a(\omega)$  should be indicative of the onset of multiple scattering.

Other criteria for determining if multiple scattering is occurring have been proposed. Dainty and Toksöz (1981) give

$$1/Q_i \ll GV/\omega \quad (15)$$

as a sufficient but not a necessary condition for multiple scattering. Sato (1977), on the other hand, gives

$$t_m > 1/(GV) \quad (16)$$

as a necessary but not a sufficient condition for multiple scattering, where  $t_m$  is the total length of the coda after origin.

The remaining theoretical question is the characterization of the scatterers, which controls the relationship between  $g(\pi, \omega)$  and  $G(\omega)$ . Previously, it had been hoped that the measurements reported here would answer this question. However, whilst they appear to shed some light on

the subject, it appears that there are too many parameters involved to allow unique interpretations. Briefly, two types of models have been used to characterize the scatterers--either bodies of a specified shape, distributed randomly (e.g., Dainty, 1981), or random fluctuations of the medium described by their autocorrelation (e.g., Wu, 1982). There are some similarities between the various models--if there is a length scale associated with the scatterers (the object size if the scatterers are modelled as bodies, or a correlation scale length for random fluctuations), then for wavelengths  $\lambda$  much longer than this length scale the scattering is weak but strongly frequency dependent, increasing as the fourth power of frequency (Rayleigh scattering). The scattered intensity increases until  $a/\lambda \sim 1$ . For media with sharp boundaries, backscattering is approximately frequency independent for  $a/\lambda \gg 1$  (geometrical scattering; Dainty, 1984), or declines rapidly if there are no sharp boundaries. Thus, if a variety of length scales of scatterers are present in the earth, the length scales that are the same order of magnitude of the wavelength or greater are likely to be important.

An important area of difference between the models, however, lies in the predicted dependence of the scattered intensity on the angle between the original wave and the scattered wave. Almost all possibilities seem to be allowed, including isotropic scattering (spheres at high frequency), strong forward scattering (acoustic velocity fluctuations at high frequency; Dainty, 1984), or strong backscattering (impedance fluctuations; Wu and Aki, 1984). At any given frequency, the angular dependence of scattering controls the ratio of the back-

scattering turbidity  $g(\pi, \omega)$  to the total turbidity  $G(\omega)$ . For the case of isotropic scattering

$$g(\pi, \omega)/G(\omega) = 1/(4\pi) \sim 10\% \quad (17)$$

Ratios of  $g(\pi, \omega)$  to  $G(\omega)$  substantially less than 0.1 (10%) would indicate a medium that predominantly scatters in the forward direction; Dainty (1984), for an acoustic medium with velocity fluctuations at high frequencies, obtains

$$g(\pi, \omega)/G(\omega) = 1/(56\pi) \sim 1\% \quad (18)$$

Likewise, ratios of  $g(\pi, \omega)$  to  $G(\omega)$  substantially greater than 0.1 would indicate a predominantly backscattering medium. Wu and Aki (1984) suggest that an elastic medium with impedance fluctuations would have these properties.

### Analysis and Results

The data used in this paper are mainly those of Duckworth (1983), with data from Dainty and Tie (1984) used for comparison purposes. Analysis methods are given in Duckworth (1983) and Dainty and Duckworth (1983). Briefly, codas are analyzed by determining the power spectrum as a function of time in a moving window 1.28 sec long for the results of Duckworth (1983), or 0.64 sec for the results of Dainty and Tie (1984). The power spectra are averaged over octave bands and then fitted as a function of time at a specified center frequency to equation (1) or equation (7) to obtain  $Q$  and  $A_b$  or  $A_s$ . Then equations (5) and (2) or (8) as appropriate were used to calculate  $G_a(\omega)$  and  $g(\pi, \omega)$ . Further, following Duckworth (1983), the coda was split into two time



sections: times less than 10 seconds after origin and times greater than 10 seconds. This followed visual examination of plots of the Monticello, South Carolina, codas as power at a frequency as a function of time. There appeared to be a change in the decay rate of the coda at about 10 seconds after origin, and separate fits were made to examine this, both on the Monticello, South Carolina, records and the Mammoth Lakes, California, records.

The records used are digital records used by Fletcher (1982) at Monticello Reservoir, South Carolina, and by Archuleta et al. (1982) at Mammoth Lakes. The digital recordings were kindly supplied by Paul Spudich of the United States Geological Survey. The seismograms are sampled at a rate of 200 samples per second with a 12 bit sample. The antialiasing filter has a corner of 50 Hz; analysis has been limited to frequencies less than this. The events and the stations used in this study are shown in Figures 1 and 2. Table 1 indicates which events and stations were used in such analysis.

Results of the analysis are shown in Figures 3 through 6. For each seismogram analyzed, both equation (1) and equation (7) were fit. The results from equation (1) will be called the "spherical" case and the results from equation (7) the "cylindrical" case. Figures 3 through 6 show average values for both  $G_a(\omega)$  and  $g(\pi, \omega)$  for each fit at Mammoth and Monticello for long ( $>10$  sec) and short ( $<10$  sec) codas. Note that results from the "spherical" case usually give lower numerical values than results from the cylindrical case, but the general trend of the data, and the relative values of  $G_a(\omega)$  and  $g(\pi, \omega)$  are similar. Earlier results of Dainty and Tie (1984) using different events and a shorter

Table 1a. Locations of earthquakes and recording stations at Monticello, South Carolina.

Event/Station	"S" Time	Range	Location
1271000			34°20.03'N 081°19.62'W
DUC	0.68	2.2	34°20.07'N 081°21.06'W
DON	1.05	3.5	34°21.42'N 081°21.20'W
LKS	0.89	3.0	34°19.95'N 081°17.69'W
1320218			NOT POSSIBLE
JAB	1.66	5.8	34°22.28'N 081°19.47'W
1281119			34°20.70'N 081°20.81'W
JAB	1.31	4.6	
1302328			34°20.49'N 081°20.65'W
SNK	0.56	1.8	34°20.29'N 081°19.54'W
JAB	1.19	3.8	
LKS	1.38	4.7	
1310603			34°18.50'N 081°20.50'W
SNK	1.05	3.7	
LKS	1.48	5.2	
JAB	2.00	7.0	
1281831			NOT POSSIBLE
JAB	1.02	3.57	

Table 1b. Locations of earthquakes and recording stations at Mammoth Lakes, California.

Event/Station	"S" Time	Range	Location	
1571941			37°32.91'N	118°52.53'W
CBR	5.50	15.2	37°40.75'N	118°49.51'W
TOM	6.11	18.0	37°33.05'N	118°40.32'W
LKM	5.97	17.3	37°41.80'N	118°56.13'W
1592317			37°37.50'N	118°52.52'W
HCF	2.38	3.0	37°38.51'N	118°50.98'W
FIS	2.58	4.2	37°36.84'N	118°49.82'W
CBR	3.60	7.5		
LKM	3.73	9.6		
MGE	4.03	10.6	37°33.67'N	118°47.22'W
LAK	5.30	13.1	37°38.49'N	118°43.70'W
TOM	6.78	19.7		
ROC	6.71	19.8	37°29.78'N	118°43.16'W

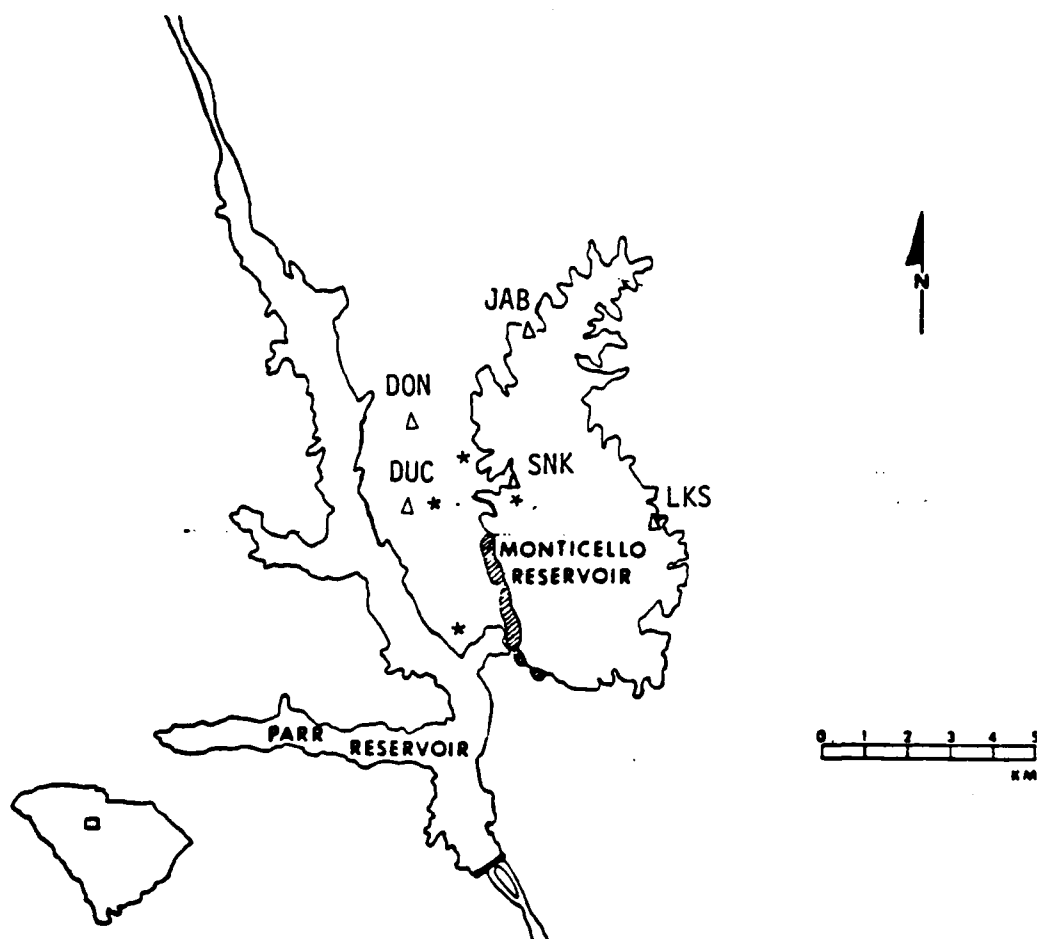


Figure 1. Recording stations and epicenters at Monticello Reservoir, South Carolina. Stations - Δ, epicenters - \*

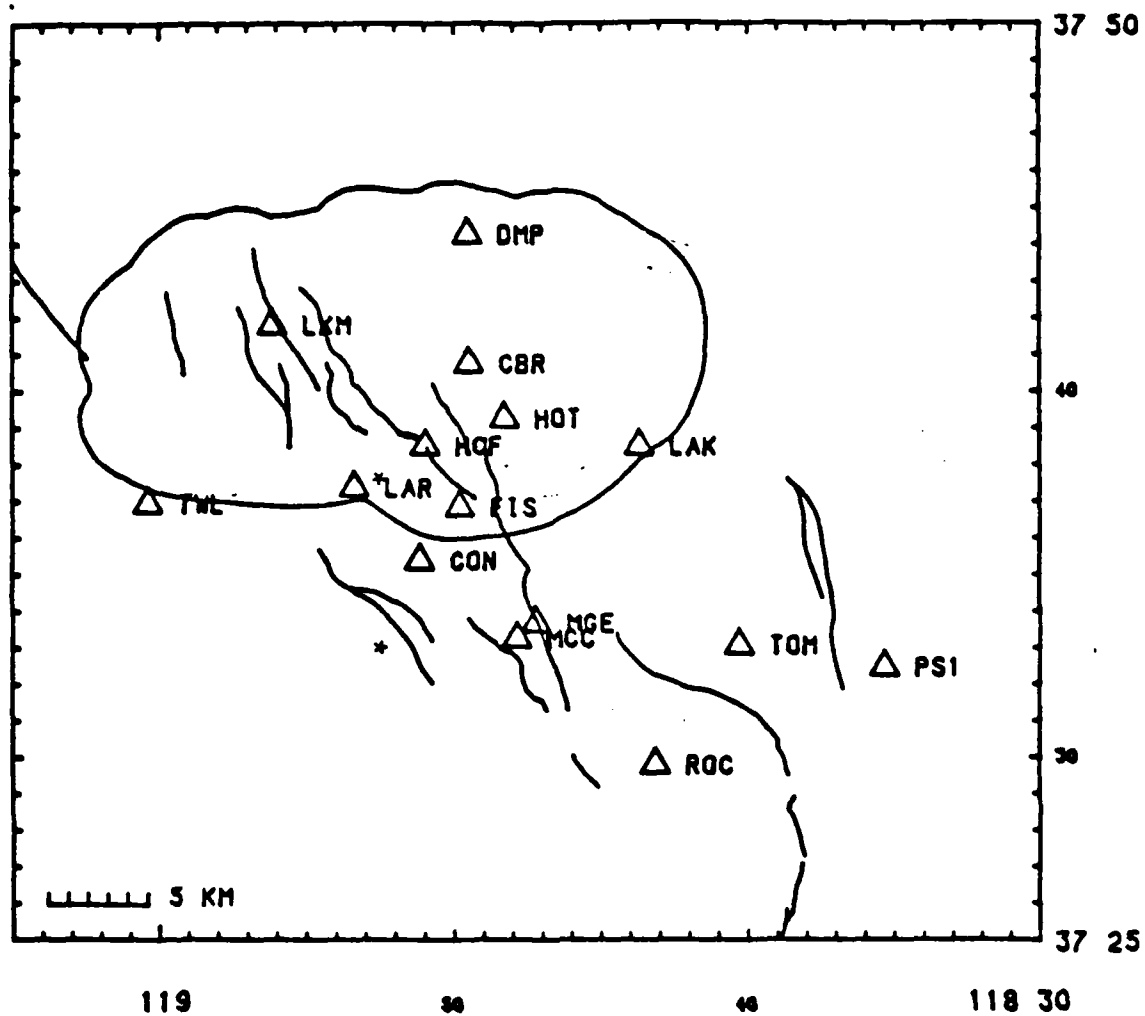


Figure 2. Recording stations and epicenters, Mammoth Lakes, California. Stations -  $\Delta$ , epicenters - \*. Outline of Long Valley Caldera and major faults shown.



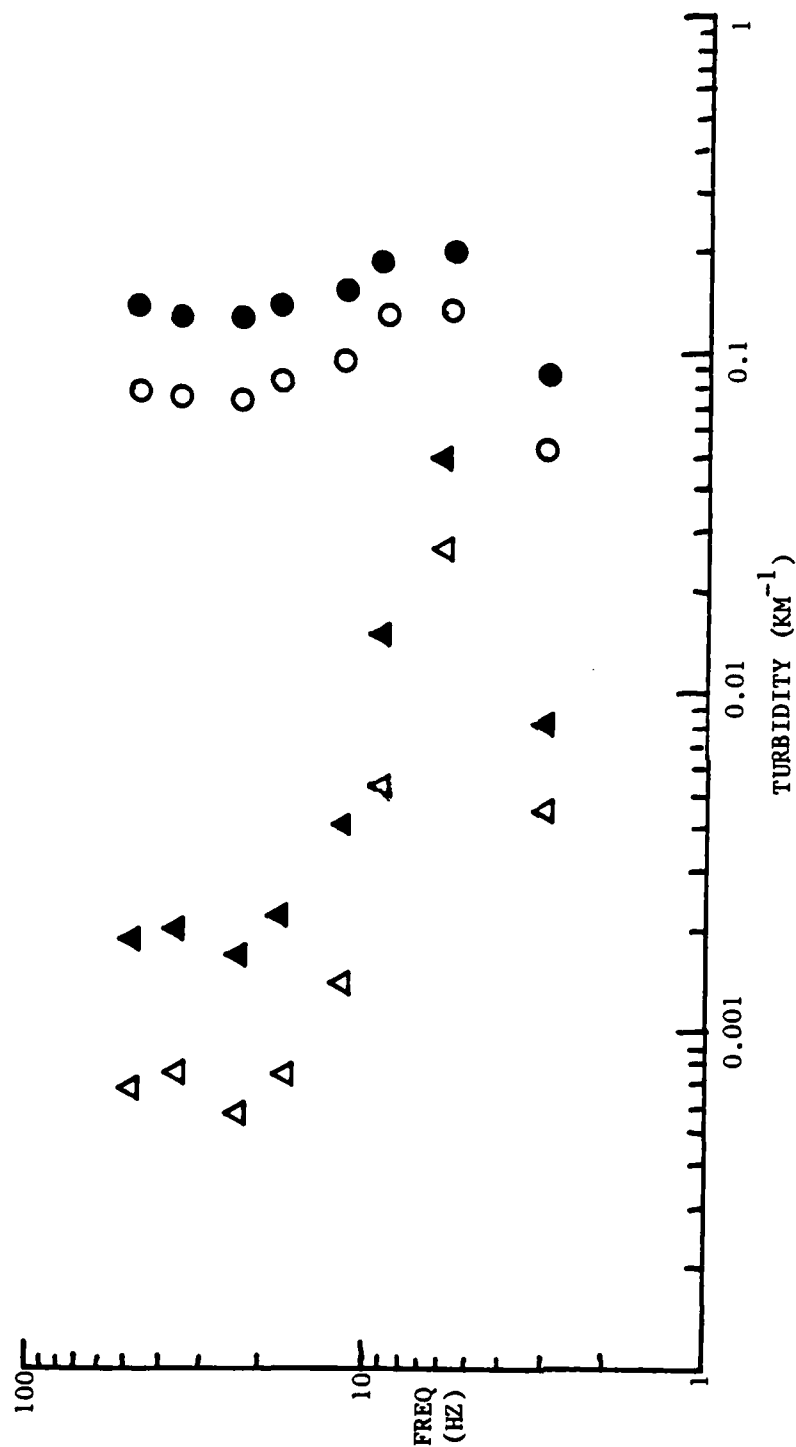


Figure 3. Total apparent turbidity ( $G_a$ ) and backscattering turbidity ( $g(\pi, \omega)$ ) as a function of frequency, Monticello, SC, for codas less than 10 seconds long. Open symbols, spherical spreading assumed, closed symbols, cylindrical spreading assumed. Circles are  $G_a$ , triangles are  $g(\pi, \omega)$ .

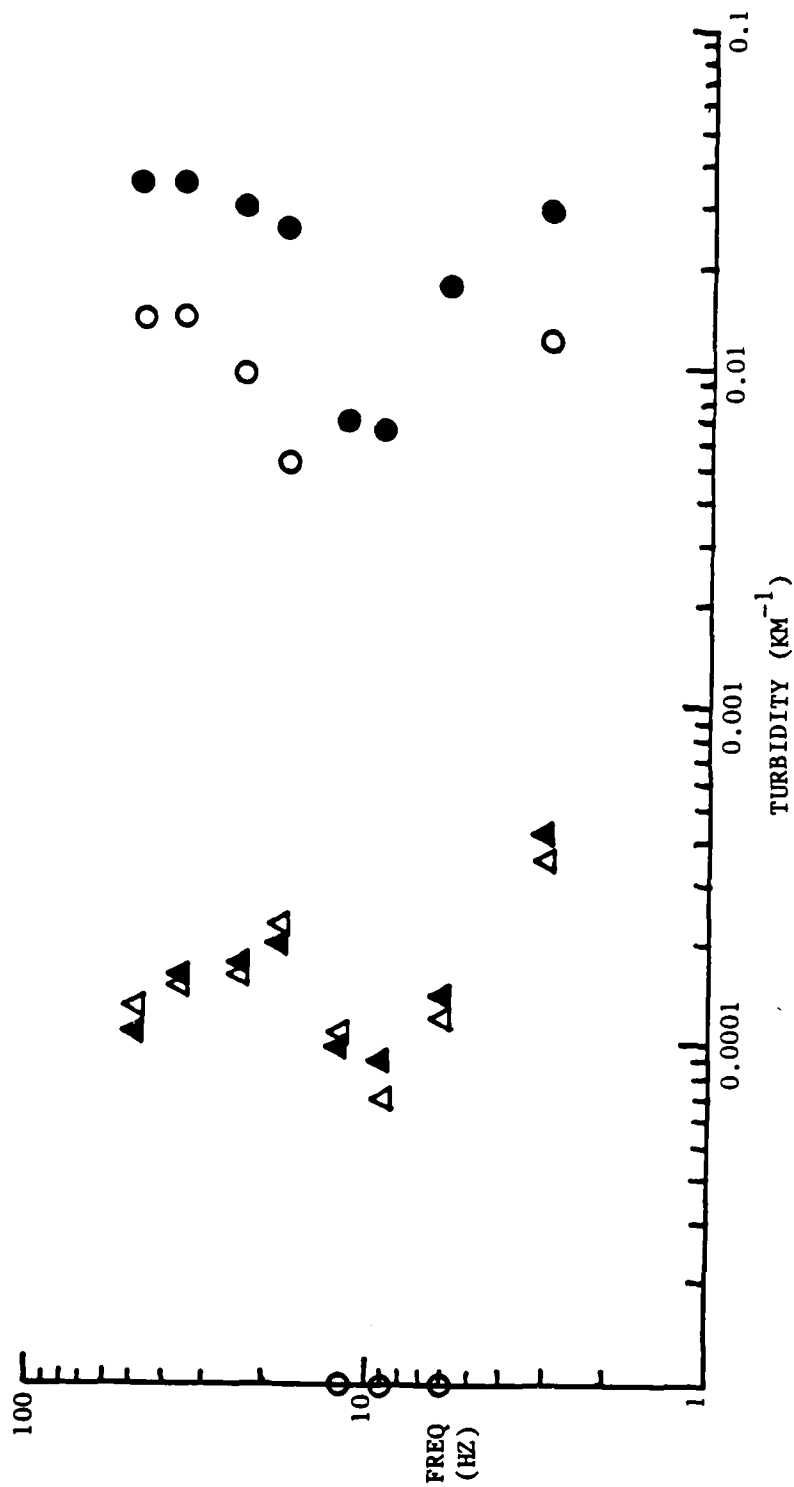


Figure 4. Total apparent turbidity and backscattering turbidity as a function of frequency, Monticello, SC, for codas more than 10 seconds long. Symbols as for Figure 3.

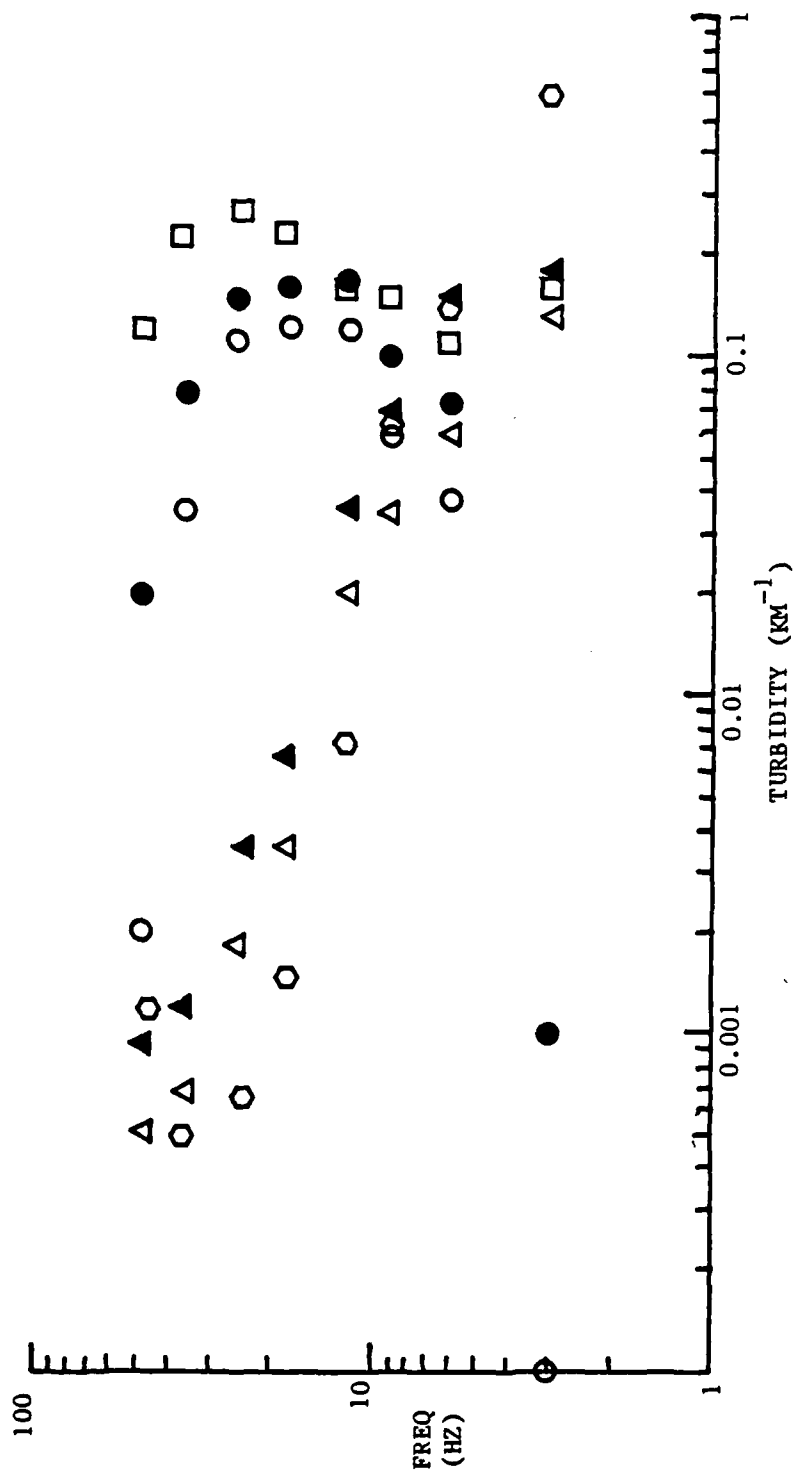


Figure 5. Total apparent turbidity and backscattering turbidity, Mammoth Lakes, CA, for codas less than 10 seconds long. Symbols as for Figure 3, plus: open squares, total apparent turbidity from Dainty and Tie (1984); open hexagons, backscattering turbidity, Dainty and Tie (1984).

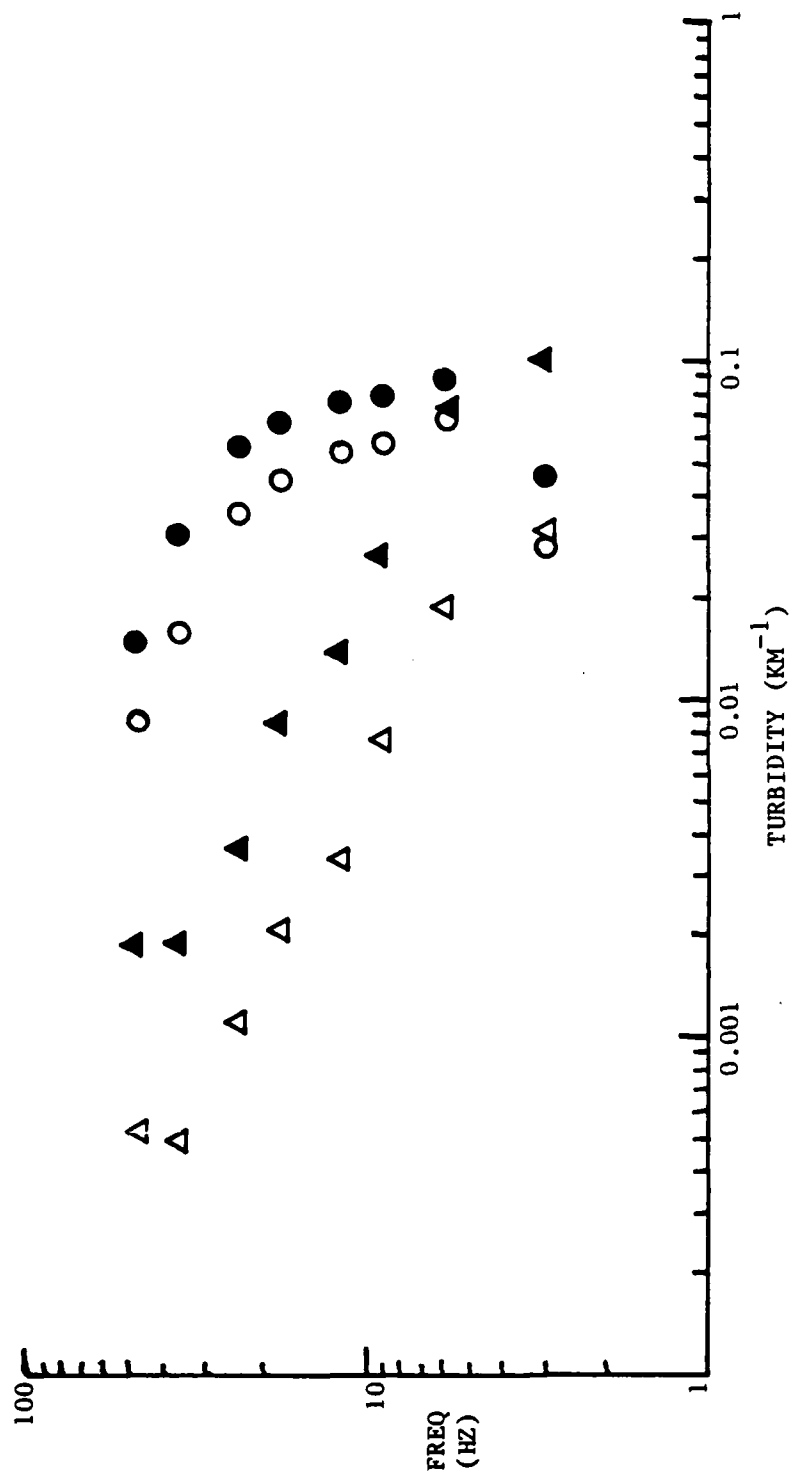


Figure 6. Total apparent turbidity and backscattering turbidity, Mammoth Lakes, CA, for codas more than 10 seconds long. Symbols as for Figure 3.

window are shown in Figure 5 for comparison; these earlier results refer to a spherical case, short coda, and were obtained from Mammoth seismograms. These results will be discussed in the next section.

Sometimes, negative values of  $Q$  were obtained when fitting equation (1), and less frequently equation (7). This indicates that the coda power at that frequency is decaying less rapidly than  $t^{-2}$  if equation (1) is being fit, or less rapidly than  $t^{-1}$  if equation (7) is being fit. Such values have been counted as  $Q \rightarrow \infty$  ( $G_a(\omega) \rightarrow 0$ ) in the averages. In the log-log plots, values of  $G_a(\omega)$  corresponding to this case in the average have been plotted at the lowest scale values.

### Discussion

The first question that will be addressed is the issue of spherical (body wave) spreading as opposed to cylindrical (surface wave) spreading of the scattered waves in the coda. In Figures 3 through 6, the results of spherical spreading fits are shown as open symbols and the results of cylindrical spreading fits as closed symbols. It appears that in most cases, an equally good fit can be obtained using either assumption. The major exception to this statement is seen in Figure 4, Monticello codas more than 10 seconds long, where negative values of  $Q$  are obtained for frequencies near 10 Hz for spherical spreading fits. This suggests that cylindrical spreading along a "channel" is responsible for the coda at Monticello after 10 seconds. Because the effect is noticeable at times as short as 10 seconds, the channel must exist in the crust within about 15 km of the surface, since the scattered energy must get from a shallow ( $\sim 1$  km deep) source to the scatterers and back to the surface receiver in as little as 10 seconds.



It is clear from the results obtained and shown in Figures 3 through 6 that multiple scattering is occurring at frequencies less than about 20 Hz in all cases except the aforementioned Monticello codas at times longer than 10 seconds. For all these cases there is a rise of the backscattering turbidity,  $g(\pi, \omega)$  for frequencies less than 20 Hz, without a corresponding rise in  $G_a(\omega)$ . Indeed, in the case of Mammoth Lakes (Figures 5 and 6),  $g(\pi, \omega)$  is greater than  $G_a(\omega)$  for the lowest frequency studied, 3 Hz. This violates equation (6) severely, and is not possible under the assumption of single scattering. A similar result was obtained by Andrews (1982). Furthermore, in the case of Mammoth Lakes the apparent total turbidity declines by at least a factor of two at 3 Hz, suggesting that at least half of the decay at higher frequencies is due to scattering. The case of Monticello codas at times longer than 10 seconds, however, seems to fit the single scattering theory well, obeying condition (16).

The nature of the scatterers may be partly determined by the data presented here. Basically, the approach is to compare the relative values of  $g(\pi, \omega)$  and  $G_a(\omega)$ . Consider first Figure 4, the data from Monticello for codas longer than 10 seconds. The backscattering turbidity  $g(\pi, \omega)$  and the apparent total turbidity  $G_a(\omega)$  show an excellent correlation with each other. When the apparent total turbidity decreases around 10 Hz, so does the backscattering turbidity. This suggests that the apparent total turbidity is mainly due to scattering and thus a close approximation to the true total turbidity  $G(\omega)$ . The value of the backscattering turbidity is about 1%, or less, than the total turbidity, which indicates a medium that mainly forward and/or

side scatters, such as a velocity fluctuation (Dainty, 1984; Wu and Aki, 1984).

The other cases examined (Figures 3, 5, and 6) are not so easy to interpret for two reasons. One is the effect of multiple scattering already noted, preventing a measure of  $g(\pi, \omega)$  and  $G(\omega)$ . This is the most serious difficulty at low frequency. At high frequencies, we note from Figure 7 that the backscattering turbidity  $g(\pi, \omega)$  has the same behavior for all three cases, quite distinct from the Monticello codas longer than 10 seconds. From Figure 7, however, the apparent total turbidity,  $G_a(\omega)$ , at Mammoth Lakes (both cases) seems to drop at frequencies above 20 Hz. This may be due to contamination by noise, which would tend to make the coda decay seem less than it really is, without affecting the determination of the backscattering turbidity  $g(\pi, \omega)$ , as suggested by Figures 7 and 8. In support of this, note (Andrews, 1984, personal communication) that there is very little energy in the Mammoth Lakes sources above 20 Hz.

If in fact the cases of the Monticello codas less than 10 seconds long and the Mammoth Lakes codas (both coda lengths) are similar, as suggested by Figure 8, we may compare the two Monticello cases of codas less than 10 seconds long (Figure 3) and greater than 10 seconds long (Figure 4). Figures 7 and 8 may also be used. We see that both  $g(\pi, \omega)$  and  $G_a(\omega)$  are a factor of 5 to 10 larger for the short codas as compared to long codas for frequencies greater than 20 Hz. This suggests that the channel in which short coda energy propagates is similar to that for long codas in its scattering properties, but scatters more strongly. At frequencies below 20 Hz, little can be said. It is possible, through

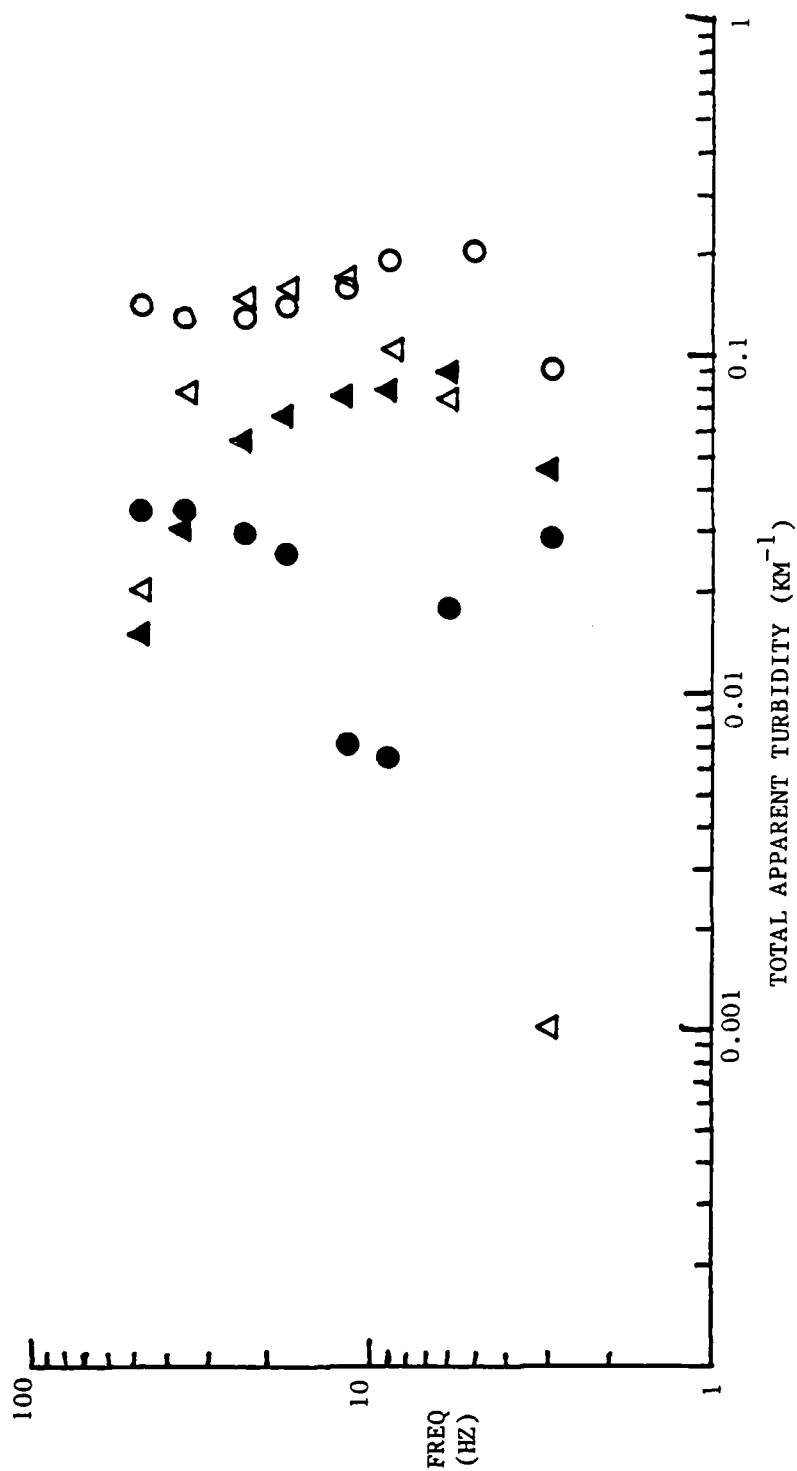


Figure 7. Total apparent turbidity, cylindrical spreading assumed. Circles, data from Monticello, SC, triangles, data from Mammoth Lakes, CA. Closed symbols, data from codas more than 10 seconds long, open symbols, data from codas less than 10 seconds long.

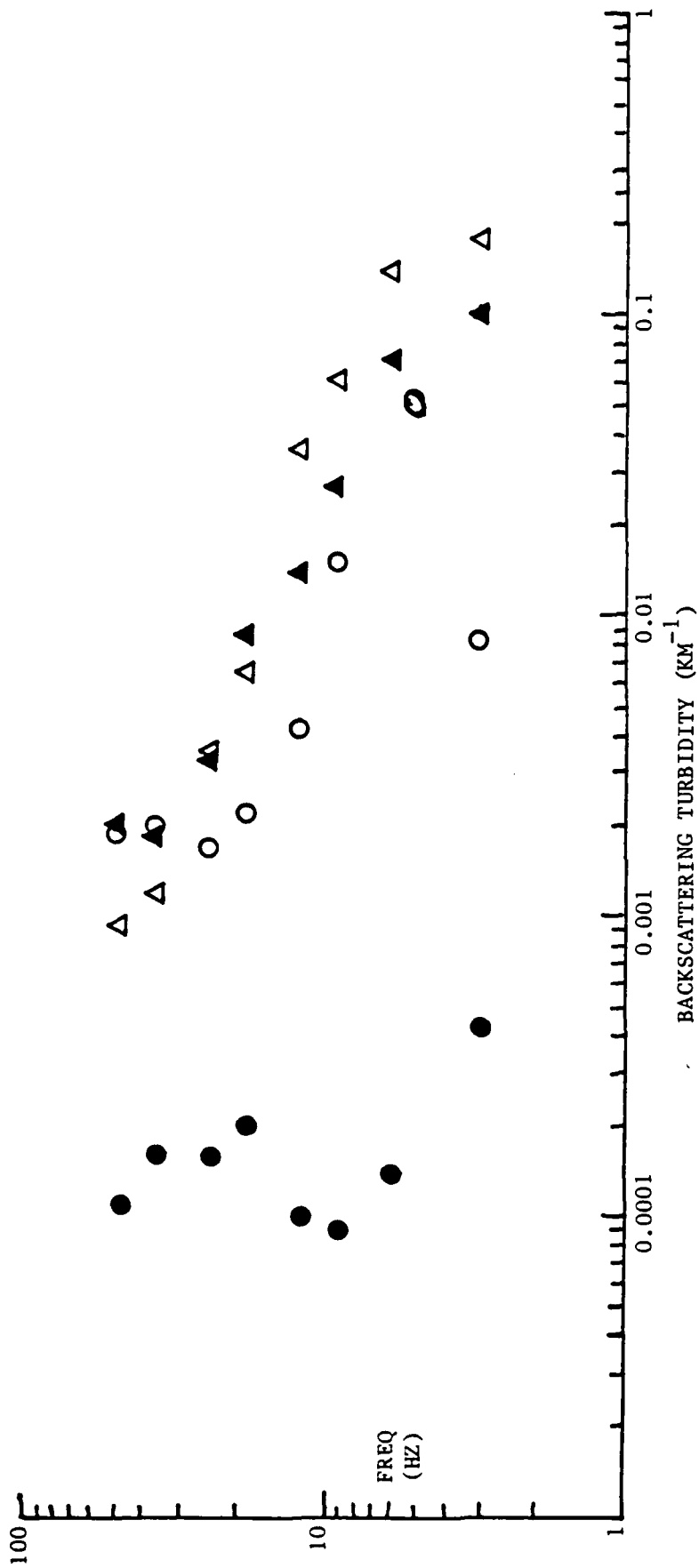


Figure 8. Backscattering turbidity, cylindrical spreading assumed. Symbols as for Figure 7.

equation (15), for the scattering properties at low frequencies to be the same as those at high frequencies, and yet for there to be multiple scattering at low frequencies ( $<20$  Hz) and not at high frequencies ( $>20$  Hz), if  $Q_i$  is around 1000. However, this is the approximate value of the total  $Q$  at high frequency ( $>20$  Hz), leaving no room for a scattering contribution. Accordingly, it seems more likely that there is a group of scatterers of size 50 m and larger causing the increased scattering implied by the rise in  $g(\pi, \omega)$  seen for codas of less than 10 seconds length at Monticello.

Finally, what is the nature of the difference in coda observed before and after 10 seconds at Monticello, South Carolina? I have interpreted this in terms of equation (10), i.e., as two different regions of the crust which scatter differently. Note that if one channel has high scattering, it will tend to dominate at short times because  $g(\pi, \omega)$ , controlling the excitation, is large, but will be negligible at long times because  $G(\omega)$ , controlling the decay, is large. Thus the short time ( $<10$  sec) coda shows the stronger scattering. Since this coda occurs immediately after the S wave, and at Mammoth Lakes does not appear to be dependent on focal depth (Tie, personal communication), I suspect that it is near surface, spherical(?) scattering. The long coda ( $>10$  sec) may represent cylindrical(?) propagation in a crustal "channel", possibly at somewhat deeper depths (10 to 15 km?).

From Figure 8 especially, it seems that there is little difference between the codas at Mammoth Lakes, both long and short, and the short ( $<10$  sec) coda at Monticello. This indicates that the upper crust is rather similar at these two tectonically very different sites. However,



at times greater than 10 seconds the Monticello coda shows evidence of much weaker scattering than at times less than 10 seconds, whereas the Mammoth Lakes data show little if any significant difference between codas in the two time ranges (Figure 8). Either the crustal low-scattering channel seen at Monticello is not present at Mammoth Lakes (the most likely conclusion) or it scatters as strongly as the near-surface channel. Because propagation in the crustal low-scattering channel is suspected to be "cylindrical", i.e., confined to the horizontal direction, it may be the same channel as that used by Lg. If this is true, the results obtained have predicted that Lg would propagate more efficiently at Monticello than at Mammoth Lakes, a prediction that is certainly true for the wider regions in which these areas are located (Nuttli, 1973). Further, the Q measured from long time codas would be representative of Lg Q (Mitchell and Nuttli, 1983).

#### Acknowledgment

Paul Spudich of the U.S. Geological Survey, Menlo Park, kindly supplied the records used in this study.

## BIBLIOGRAPHY

- Aki, K., and B. Chouet (1975). Origin of coda waves: source, attenuation and scattering effects. J. Geophys. Res., 80, 3322.
- Andrews, D. J. (1982). Shear wave and coda attenuation of two aftershocks at Mammoth Lakes, California. EOS, 63, 1029.
- Archuleta, R. J., E. Cranswick, C. Mueller, and P. Spudich (1982). Source parameters of the 1980 Mammoth Lakes, California, earthquake sequence. J. Geophys. Res., 87, 4595.
- Dainty, A. M. (1981). A scattering model to explain seismic Q observations in the lithosphere between 1 and 30 Hz. Geophys. Res. Lett., 8, 1126.
- Dainty, A. M. (1984). High frequency acoustic backscattering and seismic attenuation. J. Geophys. Res., 89, 3172.
- Dainty, A. M., and R. M. Duckworth (1983). Observations of coda Q for the crust near Mammoth Lakes, California, and Monticello, South Carolina. Semi-Annual Technical Report, Contract AFOSR-83-0037, p. 4.
- Dainty, A. M., and A. Tie (1984). Investigation of backscattering and coda decay for shallow earthquakes at Mammoth Lakes, California. Annual Technical Report, Contract AFOSR-83-0037, p. 3.
- Dainty, A. M., and M. N. Toksoz (1977). Elastic wave propagation in a highly scattering medium--a diffusion approach. J. Geophys., 43, 375.
- Dainty, A. M., and M. N. Toksoz (1981). Seismic codas on the earth and moon: a comparison. Phys. Earth Planet. Int., 26, 250.
- Duckworth, R. M. (1983). Q estimates from local coda waves. M.S. Thesis, Georgia Institute of Technology.
- Fletcher, J. B. (1982). A comparison between the tectonic stress measured in situ and stress parameters from induced seismicity at Monticello Reservoir, South Carolina. J. Geophys. Res., 87, 6031.
- Mitchell, B. J., and O. W. Nuttli (1983). Attenuation of seismic waves at regional distances. Semi-Annual Report, Contract F49620-83-C-0015.
- Nuttli, O. W. (1973). Seismic wave attenuation and magnitude relations for eastern North America. J. Geophys. Res., 78, 876.
- Sato, H. (1977). Energy propagation including scattering effects single isotropic scattering approximation. J. Phys. Earth, 25, 27.

Wu, R.-S. (1982). Attenuation of short period seismic waves due to scattering. Geophys. Res. Lett., 9, 9.

Wu, R.-S., and K. Aki (1984). Scattering of random waves by a random medium and small scale inhomogeneities in the lithosphere. Annual Technical Report, Contract F49620-82-K-0004.